Biochimica et Biophysica Acta 1788 (2009) 686–695

Contents lists available at ScienceDirect

Biochimica et Biophysica Acta

journal homepage: www.elsevier.com/locate/bbamem

Solid-state NMR and molecular dynamics simulations reveal the oligomeric ion-channels of TM2-GABA$_A$ stabilized by intermolecular hydrogen bonding

Senthil K. Kandasamy [a], Dong-Kuk Lee [b,c,1], Ravi P.R. Nanga [b,c], Jiadi Xu [b,c], Jose S. Santos [b,c], Ronald G. Larson [a], Ayyalusamy Ramamoorthy [b,c,*]

[a] Department of Chemical Engineering, University of Michigan, Ann Arbor, MI 48109-1055, USA
[b] Department of Biophysics, University of Michigan, Ann Arbor, MI 48109-1055, USA
[c] Department of Chemistry, University of Michigan, Ann Arbor, MI 48109-1055, USA

ARTICLE INFO

Article history:
Received 5 September 2008
Received in revised form 31 October 2008
Accepted 3 November 2008
Available online 21 November 2008

Keywords:
GABA receptor
Membrane protein
Ion channel
Solid state NMR
Lipid bilayer
Structure

ABSTRACT

The second transmembrane (TM2) domain of GABA$_A$ receptor forms the inner-lining surface of chloride ion-channel and plays important roles in the function of the receptor protein. In this study, we report the first structure of TM2 in lipid bilayers determined using solid-state NMR and MD simulations. The interatomic ^{13}C–^{15}N distances measured from REDOR magic angle spinning experiments on multilamellar vesicles, containing a TM2 peptide site specifically labeled with $^{13}C'$ and ^{15}N isotopes, were used to determine the secondary structure of the peptide. The ^{15}N chemical shift and ^{1}H–^{15}N dipolar coupling parameters measured from PISEMA experiments on mechanically aligned phospholipid bilayers, containing a TM2 peptide site specifically labeled with ^{15}N isotopes, under static conditions were used to determine the membrane orientation of the peptide. Our results reveal that the TM2 peptide forms an alpha helical conformation with a tilted transmembrane orientation, which is unstable as a monomer but stable as pentameric oligomers as indicated by MD simulations. Even though the peptide consists of a number of hydrophilic residues, the transmembrane folding of the peptide is stabilized by intermolecular hydrogen bondings between the side chains of Ser and Thr residues as revealed by MD simulations. The results also suggest that peptide–peptide interactions in the tilted transmembrane orientation overcome the hydrophobic mismatch between the peptide and bilayer thickness.

1. Introduction

Communication through chemical synapses depends mainly on the release of a high-concentration pulse of a neurotransmitter, its diffusion through the synaptic cleft and the activation of neurotransmitter-gated ion-channels [1–4]. The predominant inhibitory neurotransmitter of the adult central nervous system, γ-aminobutyric acid (GABA), acts by binding to GABA$_A$ receptors. GABA binds to the GABA$_A$ receptor allowing the passive flow of negatively charged chloride ions down their electrochemical gradient into neurons, thus hyperpolarizing the membrane and shutting the influence of excitatory neurotransmitter. The ligand-gated GABA$_A$ receptors play a pivotal role in the mechanism of regulation of memory consolidation, substance abuse, anesthesia, and epilepsy [1,2].

To the best of our knowledge, no high-resolution structure of GABA$_A$ has so far been reported in the literature, mainly due to the limitations of existing biophysical techniques. A model depicting the topology of the GABA$_A$ receptor protein is given in Fig. 1. It consists of four transmembrane segments and a large extracellular domain that has binding sites for various drugs and ligands. Based on the mutation and functional studies, electron microscopy images, and in analogy with the well-studied N-acetyl-choline receptor, the second transmembrane (TM2) domain of the GABA$_A$ receptor is thought to form the inner-lining surface of the ion-channel. Interestingly, the amino acid sequences of the TM2 segment of various subunits of the GABA$_A$ receptor (see Fig. 2) are highly conserved [5,6]. It has also been demonstrated that a synthetic peptide corresponding to the TM2 of GABA$_A$ forms ion channels in planar lipid bilayers, suggesting that understanding the structure of this peptide channel is likely to provide insights into the function of the receptor [7]. However, unlike other channel-forming peptide fragments of ligand-gated ion-channel receptor proteins [8,9], the amino acid sequence of the TM2 peptides of GABA$_A$ receptors consists of a large

Abbreviations: CD, circular dichroism; CP, cross polarization; DMPC, 1,2-dimyristoyl-*sn*-glycero-3-phosphatidylcholine; GABA, γ-amino butyric acid; MAS, magic angle spinning; MD, molecular dynamics; MLVs, multilamellar vesicles; NMR, nuclear magnetic resonance; PISA, polarity index slant angle; PISEMA, polarization inversion spin exchange at the magic angle; POPC, 1-palmitoyl-2-oleoyl-*sn*-glycero-3-phosphatidylcholine; POPG, 1-palmitoyl-2-oleoyl-phosphatidylglycerol; REDOR, rotational echo double resonance; RF, radio frequency; SEMA, spin exchange at the magic angle; SUV, small unilamellar vesicle; TFE, trifluoroethanol; TM, tansmembrane; TPPM, two-phase pulse-modulation

* Corresponding author. Department of Biophysics, University of Michigan, Ann Arbor, MI 48109-1055, USA. Tel.: +1 734 647 6572.
E-mail address: ramamoor@umich.edu (A. Ramamoorthy).
[1] Present address: Seoul National University of Technology, Department of Fine Chemistry, Seoul, Republic of Korea.

0005-2736/$ – see front matter © 2008 Elsevier B.V. All rights reserved.
doi:10.1016/j.bbamem.2008.11.009

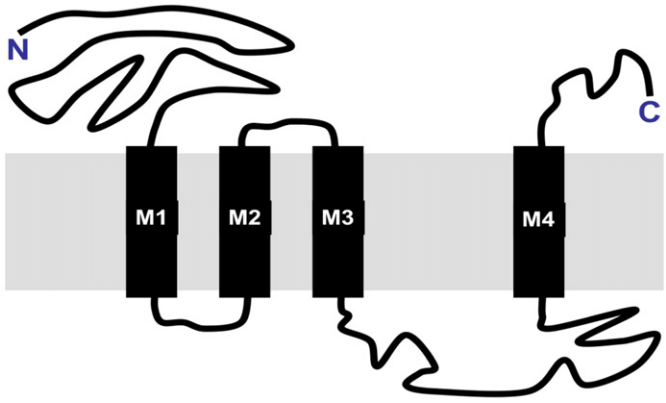

Fig. 1. A model depicting the topology of the $GABA_A$ receptor. M1, M2, M3 and M4 are the transmembrane (TM) domains of the protein.

number of hydrophilic residues (like Ser, Thr and Arg) that lead to a non-amphipathic structure in a helical geometry (Fig. 3). Thus, it is surprising that the peptide prefers to be inserted in a lipid bilayer to form ion channels even though it is neither entirely hydrophobic nor is it amphipathic. Therefore, we thought solving the high-resolution structure of the peptide in phospholipid bilayers would provide insights into the folding and ion-channel activity of the peptide in membranes.

In this study, we investigated the backbone conformation of a TM2 peptide using CD (circular dichroism) experiments on detergent micelles and small unilamellar vesicles (SUVs) at a low concentration of the peptide. REDOR (rotational echo double resonance) [10] magic angle spinning (MAS) solid-state NMR experiments were performed to measure several ^{13}C–^{15}N distances from ^{13}C and ^{15}N-double labeled TM2 peptides embedded in MLVs. The orientation of the helical structure of the peptide was measured using PISEMA (polarization inversion spin exchange at the magic angle) [11,12] solid-state NMR experiments on mechanically aligned bilayers under static experimental conditions. PISEMA experimental results suggested that the helical TM2 peptide has a transmembrane orientation irrespective of the thickness of the lipid bilayer used in our study. This observation suggests that peptide–peptide interactions dominate the hydrophobic mismatch between the hydrophobic length of TM2 and the hydrophobic thickness of the lipid bilayer. Molecular dynamics (MD) simulations of lipid bilayers containing the TM2 (α1 sequence same as α2, α3, or α5) peptide provided additional insights into the favorable peptide–peptide interactions that drive oligomerization of the peptide.

2. Materials and methods

2.1. Materials

All phospholipids (POPG (1-palmitoyl-2-oleoyl-phosphatidylglycerol), POPC (1-palmitoyl-2-oleoyl-phosphatidylcholine), and DMPC (1,2-dimyristoyl-phosphatidylcholine)) were purchased from Avanti Polar Lipids (Alabaster, AL). Chloroform and methanol were purchased from Aldrich Chemical Inc. (Milwaukee, WI). Naphthalene was purchased from Fisher Scientific (Pittsburgh, PA). All protected (unlabeled) amino acids were purchased from Bachem, Synthetech, and Protein Technologies. All amino acids with isotope labels were purchased from Cambridge isotope Laboratories (Andover, MA). Coupling agents and resin were purchased from Bachem. Solvents and deprotecting agents were obtained from Fisher Scientific and Aldrich Chemical Co. All the chemicals were used without further purification.

2.2. Synthesis

TM2 (α1 sequence same as α2, α3, or α5) peptides with and without isotopic (^{15}N or ^{15}N and ^{13}C) labels were synthesized by automated solid phase methods using standard Fmoc (9-Fluorenylmethoxycarbonyl) chemistry [7]. The crude peptides were purified by reverse-phase HPLC. The peptides were shown to be >97% pure by HPLC and MALDI.

2.3. Circular dichroism spectroscopy

Small unilamellar vesicles (SUVs) were prepared by sonication. 10 mM HEPES buffer (150 mM NaCl, 0.1 mM EDTA, pH 7.4) was added to dry lipid film and subjected to vortex and sonication to obtain a clear dispersion of SUVs. CD spectra were recorded (AVIV CD spectropolarimeter, Lakewood, NJ) at 37 °C using samples with peptide/lipid ratios 1:100 and 1:200 over the range from 200 to 250 nm. A 1.0 mm quartz cuvette was used for measurements. Contributions from the buffer and SUVs were removed by subtracting the spectra of corresponding control samples without peptide. The resultant spectra were normalized for path length and concentration.

2.4. Preparation of multilamellar vesicles for solid-state NMR experiments

Multilamellar vesicles (or unaligned bilayers) samples for MAS experiments were prepared by codissolving the required amount of peptide and typically 50 mg of lipids in 2:1 chloroform:methanol, drying under a steady stream of N_2 gas for ~30 min, and lyophilizing it overnight to remove any residual solvents. The dry lipid/peptide mixture was resuspended in 50 wt.% HEPES buffer (5 mM EDTA, 30 mM HEPES, 20 mM NaCl, pH 7.0) by heating in a water bath at 45 °C. The sample was gently vortexed for 3 to 5 min and freeze-thawed using liquid nitrogen several times to obtain a uniform mixture of lipid and peptide. All MLVs were stored at −20 °C prior to use. Before and after performing REDOR [10] experiments on MLVs (multilamellar vesicles) containing 3 mol% peptide, ^{31}P chemical shifts were measured to confirm the lamellar phase liquid crystalline nature of the sample. ^{31}P experiments were also carried out on MLVs containing an unlabeled peptide concentration up to 7 mol% to confirm the absence of any peptide-induced changes in lamellar phase lipid structures.

While the solubility of the peptide and lipids was much better when a small amount of TFE (trifluoroethanol) was used, it was very difficult to completely remove TFE from the sample and therefore we avoided TFE in the sample preparation. In fact, ^{31}P CSA (chemical shift anisotropy) span of MLVs (with no peptide) prepared using TFE was different from the values obtained from samples that were prepared without using TFE. This could presumably because the presence of a trace amount of TFE solvent in the sample (even after 12 h of lyophilization) could alter the electronic environment around ^{31}P nuclei of lipids and possibly the lipid bilayer properties. Therefore, one must be cautious about the use of fluorinated solvents like TFE or TFA in the preparation of model membranes.

2.5. Preparation of mechanically aligned bilayers for solid-state NMR experiments

Stock solutions were prepared by mixing the desired molar amounts of lipids (typically 80 mg) and peptide in 2:1 chloroform: methanol solution and naphthalene (lipid:naphthalene 4:1 molar ratio) [13]. Small volumes (~100 μL) of each mixture were pipetted

Fig. 2. Amino acid sequences of the second transmembrane (TM2) segment of different subunits of the $GABA_A$ receptor.

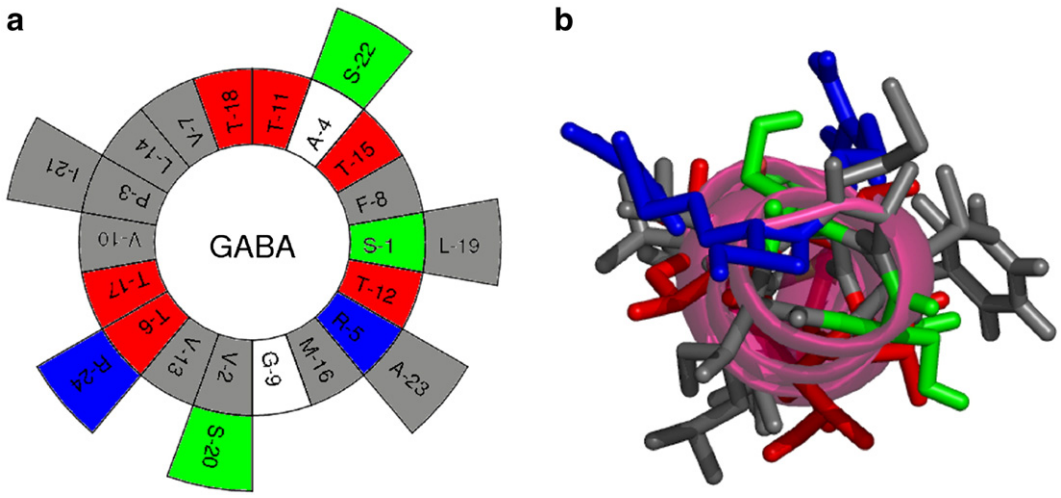

Fig. 3. Helical wheel diagram (left) and a helical structure (right) of the $GABA_A$-TM2. While CD and NMR experimental results indicate that the peptide forms a helix in membranes, the helical representation of the peptide indicates that the peptide is not amphipathic. The arginine residues are shown in blue, the serine residues in green and the threonine residues in red.

onto 15–20 glass plates (11 mm×22 mm×50 μm, Paul Marienfeld GmbH and Co., Bad Mergentheim, Germany), allowed to dry, and then placed under vacuum overnight at 35 °C to completely remove any residual solvents and naphthalene. Small amount of water was added on the dried samples and then they were placed for approximately seventy hours in a hydration chamber at 95% relative humidity, which is maintained above a saturated ammonium phosphate solution. The glass plates were stacked, wrapped with parafilm, and sealed in polyethylene bags to avoid dehydration during for NMR experiments.

2.6. NMR experiments

All solid-state NMR experiments were performed using a Varian/Chemagnetics 400 MHz spectrometer with ^{1}H, ^{31}P, ^{13}C and ^{15}N resonance frequencies of 400.138, 161.979, 100.8, and 40.55 MHz, respectively. A home-built, double-resonance, flat-coil probe was used for mechanically aligned samples, while a 5 mm triple-resonance MAS probe was used for MAS experiments on MLVs. In the case of aligned samples, the lipid bilayers were positioned with the bilayer normal parallel to the external magnetic field of the NMR spectrometer. ^{15}N chemical shift spectra of labeled peptides from mechanically aligned samples were recorded using a ramped cross-polarization (ramp-CP) [14] sequence with a ^{1}H π/2 pulse length of 3 μs, 62.5 kHz CP RF (radio frequency) power, and a 80 kHz two-phase pulse-modulation (TPPM) [15] decoupling of protons during acquisition at 37 °C. Typically >4000 scans were acquired to obtain a reasonable signal-to-noise 1D ^{15}N chemical shift spectrum using a 1 ms contact time for the ramp-CP with a 10 kHz ramp on the ^{1}H channel and a recycle delay of 3 s.

^{31}P chemical shift spectra of aligned samples were obtained using a chemical shift echo sequence, 90°–τ–180°–τ–acq, with τ=100 μs and 35 kHz ^{1}H decoupling. The spectra of oriented samples were referenced with respect to 85% H_3PO_4 between glass plates (0 ppm) [13]. These spectra confirmed that the samples were well aligned and the peptides do not induce any non-lamellar phase structures of lipids due to the peptide–lipid interaction. A representative ^{31}P chemical shift spectrum is given in Fig. 4. Typical ^{31}P π/2 pulse lengths were 3.0–3.5 μs and the spectral width was 50 kHz. About 512 transients were averaged with a recycle delay of 3 s. The FID was processed beginning at the top of the echo with a 100 Hz exponential broadening, zero filled to 4096 points, and Fourier transformed. All NMR spectra were collected at 37 °C.

2D PISEMA experiments were performed on mechanically aligned samples containing ~5 mg of a ^{15}N labeled peptide as explained in the literature [12]. A 50 kHz RF field was used in the ^{1}H channel at on-resonance during the preparation 90° pulse and rampCP, and a 35.355 kHz offset during the Lee–Goldburg [16] sequence in the t_1 period (or during the SEMA (spin exchange at the magic angle) sequence) of PISEMA [17,18]. 50 and 61.2 kHz RF field strengths were used to spin-lock the ^{15}N magnetization during ramp-CP and SEMA respectively. Protons were decoupled using the TPPM sequence with an 80 kHz RF field during the ^{15}N signal acquisition. Typically 2000 scans and 48 t_1 experiments with a recycle delay of 3 s were used to obtain a 2D spectrum of the sample. Because of the low signal-to-noise ratio from bilayer samples, the experimental conditions were first optimized on a single crystal of n-acetyl-L-^{15}N-valyl-L-^{15}N-leucine. The optimized experimental conditions were further optimized on a mechanically aligned POPC bilayers containing the TM2 peptide by carrying out several one-dimensional experiments using the regular PISEMA sequence but for different t_1 time intervals. Since the use of a high RF power in the PISEMA experiment could dehydrate the bilayer sample, air was circulated in the probe to maintain the temperature of the sample at 37 °C. In addition, the quality of aligned samples was examined using 1D ^{31}P experiments before and after PISEMA experiments. Data processing was accomplished using the Spinsight software (Varian) on a Sun Sparc workstation.

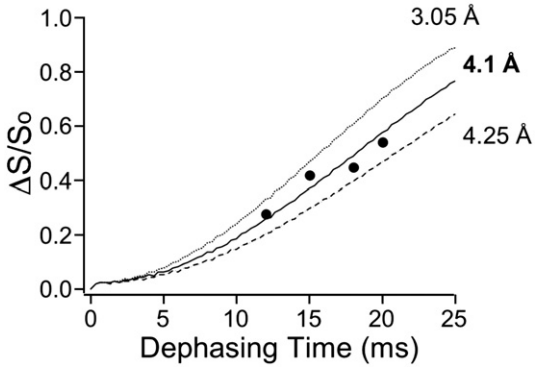

Fig. 4. A plot of $\Delta S/S_0$ against the dephasing time for POPC multilamellar vesicles containing a 3 mol% $GABA_A$-TM2 peptide labeled with ^{13}C isotope at the carbonyl carbon of Gly9 residue and ^{15}N isotope at the amide site of the Val13 residue. Experimental data points were obtained from REDOR experiments as explained in the text and the best-fit curve indicating the C′–N interatomic distance to be 4.1 Å.

2.7. Magic angle spinning solid-state NMR experiments

^{13}C chemical shift values were referred to 176.03 ppm for the isotropic chemical shift of the carboxyl carbon of glycine powder sample under MAS from that for tetramethylsilane. The ^{15}N rotational-echo double-resonance (REDOR) spectra were measured using a *XY*-8 pulse phase cycling scheme to suppress the experimental imperfections such as RF field inhomogeneity for ^{13}C nuclei, offset effects, and flip angle errors of pulses. The lengths of 180° pulses in the REDOR sequence 10 were 12.3 and 13.5 μs for ^{13}C and ^{15}N nuclei, respectively, whereas a 65 kHz RF field strength was used to decouple protons under a 4 kHz MAS. Spectra were recorded with rotor-synchronized dephasing pulses (S) and without (S_0) at various $n\tau_R$ values from 6 to 24 ms; where n and τ_R are the number of rotor cycles and rotor period, respectively. To determine the ^{13}C–^{15}N interatomic distance, the experimentally measured normalized REDOR differences, (that is $(S_0-S)/S_0$) were plotted against the $n\tau_R$ values, and the data were fit to the theoretically obtained curves.

2.8. Structure calculations

The peptide structural ensemble was calculated starting from an extended structure using the simulated annealing protocol available in NIH-XPLOR software package to generate 100 conformers (initial temperature of 3000 K with 18,000 high temperature steps, 9000 cooling steps and a step size of 2 fs) [19,20]. Final refinement of the structure ensemble was calculated at an initial temperature of 500 K with 20,000 cooling steps at a step size of 3 fs. The analysis was carried out using the "accept.inp" routine included in the NIH-XPLOR software package for no NOE violations of >0.5 Å, no dihedral angle restraint violations of >5°, no rms difference for bond deviations from ideality >0.01 and no rms difference for angle deviations from ideality >2°. The ensemble of peptide structures thus obtained was further analyzed using MOLMOL [21].

2.9. Molecular dynamics simulations

We studied three different peptide configurations, monomeric, dimeric and pentameric, inserted into two different bilayers for a total of six simulations. We used the GROMACS simulation tool [22,23] for all our simulations performed on an in-house Linux cluster 'United'. Atom lipid parameters were adapted from the work of Berger and coworkers [24]. We used the GROMOS-43a2 force field for the peptides. The starting structures for the lipid bilayers were chosen from well-equilibrated DMPC (1,2-dimyristoyl-*sn*-glycero-3-phosphatidylcholine) and POPC bilayer simulations. Both the POPC and DMPC bilayers had 128 lipids each, 64 per leaflet and ~4000 water molecules each. To create the 3:1 POPC/POPG bilayer, 16 randomly picked lipids from each leaflet of the POPC bilayer were mutated to yield POPG lipids. After the mutation, a 50 ns equilibration run was performed to equilibrate the bilayer.

Since the putative structure of the $GABA_A$ peptide is helical, an ideal helix of the peptide was created using the software Swiss PDB viewer (http://ca.expasy.org/spdbv/). This helix was solvated in a bath of water and a 5 ns-simulation was performed, with restraints on the backbone atoms. This ensured that the side chains were properly relaxed and did not retain a biased, ideal configuration. This peptide was then inserted into the equilibrated DMPC and POPC/POPG bilayers using the hole protocol developed by Faraldo-Gomez et al. [25]. Before insertion, the peptide was oriented so that the helical axis of the peptide was parallel to the bilayer normal and the center of mass of the peptide was aligned with the center of mass of the lipid bilayer.

To create the dimer, a second copy of the peptide was inserted in a parallel orientation next to the existing monomer, which was restrained. The amino acid sequence of the $GABA_A$-TM2 peptide (see Fig. 2) consists of two charged Arg residues and several polar Ser and Thr residues. In its helical conformation, the peptide is not amphipathic, with the polar and hydrophobic residues distributed fairly uniformly around the helical projection of the peptide (Fig. 3). Thus it is not easy to predict preferred peptide–peptide contacts in oligomers. The second peptide was rotated by a random degree about its own helical axis before insertion, so that the surface contact between the two peptides is random. Ideally, for unbiased predictions from these dimer simulations, several such dimers should be constructed, to fully sample all possible peptide–peptide contacts. However, due to computational limitations, only one dimer was constructed per lipid bilayer. To create the initial structure of the pentamer, a different strategy was employed. Instead of randomly placing the peptides in a pentameric bundle, a template from a homology modeled structure of the $GABA_A$ receptor was used [26]. The coordinates of the putative transmembrane domain was extracted from the coordinates of the full protein and was inserted in to both the DMPC and POPC/POPG bilayers, using the same protocol as used for the monomer and dimer.

The three peptide configurations (monomer, dimer and pentamer), inserted in two different lipid bilayers (DMPC and POPC/POPG) yielded a total of 6 simulations, details of which are listed in Table 1. After insertion, a 5 ns restrained MD simulation was performed during which the peptide backbone atoms were harmonically constrained, to allow the lipids to relax around the peptides. After 5 ns, the constraints were released and production runs of 50 ns were performed for each of the simulations. Two of the simulations (see Table 1) were extended to 100 ns, for improved sampling. The simulations were performed in an NPT ensemble, with the temperature coupled to a Berendsen thermostat at 310 K with a coupling constant of 0.1 ps. The pressure was coupled semi-isotropically to a Berendsen barostat at 1 atm, with a coupling constant of 1 ps. Both the short-range electrostatic and van der Waals interactions used a short-range cutoff of 1.2 nm and the long-range electrostatics were calculated using the PME algorithm. The trajectories were saved every picosecond and subsequently used in analysis. Data visualization was done using pymol (www.pymol.org).

3. Results

3.1. Secondary structure of GABA-TM2

3.1.1. Circular dichroism experiments

CD experiments were performed on SUVs of DMPC or POPC and SDS micelles containing a 1 mol% TM2 peptide at 37 °C. CD spectra of all of these model membrane samples were similar and characterized by the double minima at 208 and 222 nm, attributable to a helical conformation (data not shown). All peptides were assumed to be completely bound to lipid vesicles at the concentration used in the present study, as the spectra do not change upon increasing the lipid–peptide ratio.

3.1.2. REDOR NMR experiments

MLVs containing a TM2 peptide double labeled with ^{13}C at the carbonyl carbon and ^{15}N labeled at the amide-nitrogen was used at −20 °C under a 4 kHz MAS. Carbon–^{13}C chemical shifts are sensitive to secondary structure of the peptide. Measured isotropic ^{13}C chemical

Table 1
Details of the molecular dynamics simulations on lipid bilayers containing TM2 peptides of $GABA_A$ receptor

Simulations	Lipid	Number of TM2 peptides	Time (ns)
Simulation-1	DMPC	1	100
Simulation-2	POPC/POPG	1	50
Simulation-3	DMPC	2	100
Simulation-4	POPC/POPG	2	50
Simulation-5	DMPC	5	50
Simulation-6	POPC/POPG	5	50

Table 2
Interatomic distances measured from ^{13}C and ^{15}N labeled TM2 peptides of $GABA_A$ receptor embedded in POPC multilamellar vesicles using REDOR experiments under MAS

Labeled peptides	$r_{C'N}$	α-helix	β-sheet
Ala4($^{13}C'$)-Phe8(^{15}N)	4.1±0.1 Å	4.01	10.98
Val7($^{13}C'$)-Val10(^{15}N)	3.8±0.1 Å	3.76	7.66
Gly9($^{13}C'$)-Val13(^{15}N)	4.1±0.1 Å	4.01	10.98
Leu19($^{13}C'$)-Ala23(^{15}N)	4.3±0.2 Å	4.01	10.98

Distances for an alpha-helix and beta-sheet structures are also given in the table for comparison.

shift values 178.6, 179, 175.7 and 177 ppm for carbonyl carbons of Ala4, Val7, Gly9 and Leu19 suggest a helical conformation for the peptide [27,28]. To obtain a high-resolution structure of the TM2 peptide, interatomic distance between the carbonyl carbon of a residue and amide-nitrogen of another residue in the TM2 peptide was measured by using the REDOR experiment as explained in the experimental section. ^{15}N-REDOR (that is with the dephasing pulses) and full echo (that is without the dephasing pulses) spectra were obtained. The $(S_0-S)/S_0$ values were determined from the experimental spectra and plotted as shown in Fig. 4. By comparing the experimental data with the best-fitting REDOR curves [10,29], the interatomic distances were determined for each double-labeled GABA-TM2 peptide (Table 2).

A high-resolution three-dimensional structure of the TM2 peptide was obtained using the experimentally measured C–N distances as mentioned in the structure calculations in the previous section. Residues in the region between 13 and 19, for which no experimental data are available, were constrained in a helical conformation. During the first stage of simulated annealing, the backbone conformation of the peptide was constrained using the hydrogen bonding restraints (i to i+4). During the second stage of refinement, additional distance restraints obtained from solid-state NMR experiments were included. Sixteen out of the hundred refined structures passed the accept.inp routine included in the NIH-XPLOR software package. Eight lowest energy structures were further analyzed and the global backbone and heavy atom RMSD of the peptide were 0.55±0.11 and 1.36±0.25 Å, respectively, as shown in Fig. 5. It is evident that the alpha helical structure of the peptide is neither perfectly amphipathic nor completely hydrophobic (Fig. 5). Therefore, it would be interesting

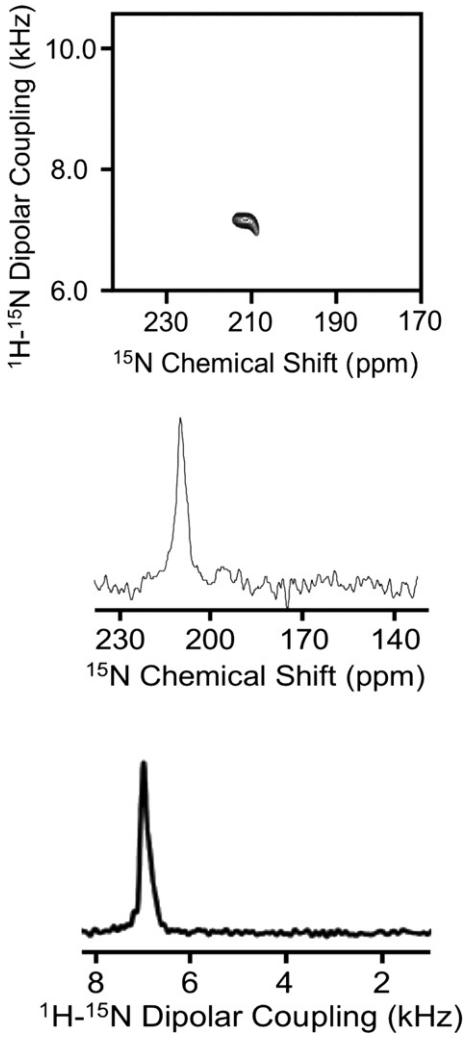

Fig. 6. 2D PISEMA spectrum (top) of aligned POPC sample containing 3 mol% of $GABA_A$-TM2 at 37 °C with the bilayer normal oriented parallel to the external magnetic field. ^{15}N chemical shift (middle) and ^1H–^{15}N dipolar coupling (bottom) spectral slices are given.

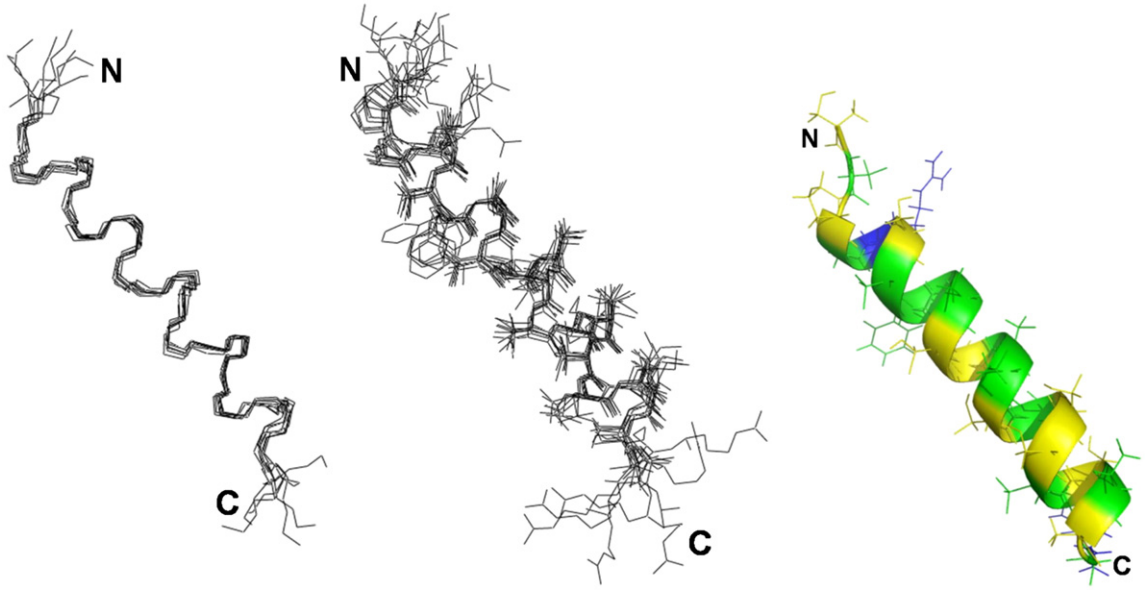

Fig. 5. Overlay of structures of $GABA_A$-TM2 calculated using solid-state NMR distance constraints as outlined in the text: backbone (left), heavy representation (middle), and the secondary structure representation (right; hydrophobic residues are shown in green while hydrophillic residues are shown in yellow (S, T and P) and blue (R) colors).

to determine the membrane orientation of the TM2 peptide using solid-state NMR experiments as explained below.

3.2. Orientation of TM2 in lipid bilayers

3.2.1. Solid-state NMR experiments on mechanically aligned lipid bilayers

Several $GABA_A$-TM2 peptides labeled with ^{15}N isotope at a single amide site were synthesized. After confirming the alignment of each mechanically aligned lipid bilayer sample using the ^{31}P NMR experiment (data not shown), ^{15}N chemical shift spectra were recorded. Once the experimental conditions were optimized using 1D ^{15}N rampCP experiments, 2D PISEMA solid-state NMR experiments were performed to measure the ^{15}N chemical shift and ^{1}H–^{15}N dipolar coupling values for several different $GABA_A$-TM2 peptides each labeled with a single ^{15}N isotope at an amide site. Observation of a single resonance in the PISEMA spectrum corresponding to a ^{15}N chemical shift value in the region 180–215 ppm and a ^{1}H–^{15}N dipolar coupling of 6–10 kHz suggests that the TM2 helical peptide has a transmembrane orientation (a representative spectrum is given in Fig. 6). The high-resolution spectral slices shown in Fig. 6 suggest that the peptides were well-aligned and immobilized in lipid bilayers and 2D PISEMA spectra are of high quality. For clarity, these experimental parameters measured from $GABA_A$-TM2 peptides are plotted in Fig. 7 along with simulated PISA (polarity index slant angle) [12,30,31] wheel PISEMA spectra. Experimental error bars estimated from the line widths in chemical shift and dipolar coupling dimensions of 2D PISEMA spectra are given in Fig. 7. As seen from simulations, the shape of PISA wheels is quite sensitive to the order parameter of the peptide. The comparison of the simulated and experimental results suggests that the GABA-TM2 peptide is tilted ~13° away from the bilayer normal and the order parameter is ~0.88 (Fig. 7). However, the shape of the PISA wheel and the measured tilt angle for the peptide could depend on other parameters like the values of the principal components of CSA tensor and molecular motions. In the simulations (Figs. 7A–C), we have used experimentally measured ^{15}N CSA tensor values from a N-acetyl-L-valyl-L-leucine dipeptide: δ_{11}=58 ppm, δ_{22}=70 ppm, and δ_{33}=230 ppm relative to liquid ammonia (0 ppm) at 25 °C [32,33]. The dependence of the shape of PISA wheels on these CSA tensor values was also simulated (Figs. 7D–F). The simulations suggest that the PISA wheel does not depend on the values of δ_{11} and δ_{22}, while it depends on the value of the least shielded CSA principal component, δ_{33}. However, the close orientation of the axis to the backbone amide-N–H bond, which is well hydrogen bonded with the carbonyl axis in the backbone of the peptide, like in the NAVL dipeptide, it is unlikely that the value of δ_{33} for the TM2 peptide would be very different from that measured from NAVL. On the other hand, though the peptide is highly immobile as suggested by the order parameter 0.88, the rotational motion of the helix could reduce the CSA values for the peptide. But the near collinearity of the rotational motion of the helix and the δ_{33} axis suggest that this is unlikely. Even if some influence of the motion and a reduced δ_{33} value for the peptide were taken into account, as suggested by simulations in Fig. 7, the value for the tilt angle could increase by a couple of degrees from the best-fit value (that is 13°). Therefore, it is reasonable to expect that the measured tilt angle of the peptide could be within 13 to 17° range. So, the tilt angle from experiments is estimated to be 15±2°.

These solid-state NMR experiments were also performed on samples with a different lipid composition to understand if the orientation of the helix changes with the thickness of the lipid bilayer. Interestingly, the tilt angle of the GABA-TM2 peptide measured from POPC, DMPC or POPC:POPG bilayers were the same within experimental errors. These results suggest that the membrane orientation of the peptide neither depends on the lipid bilayer

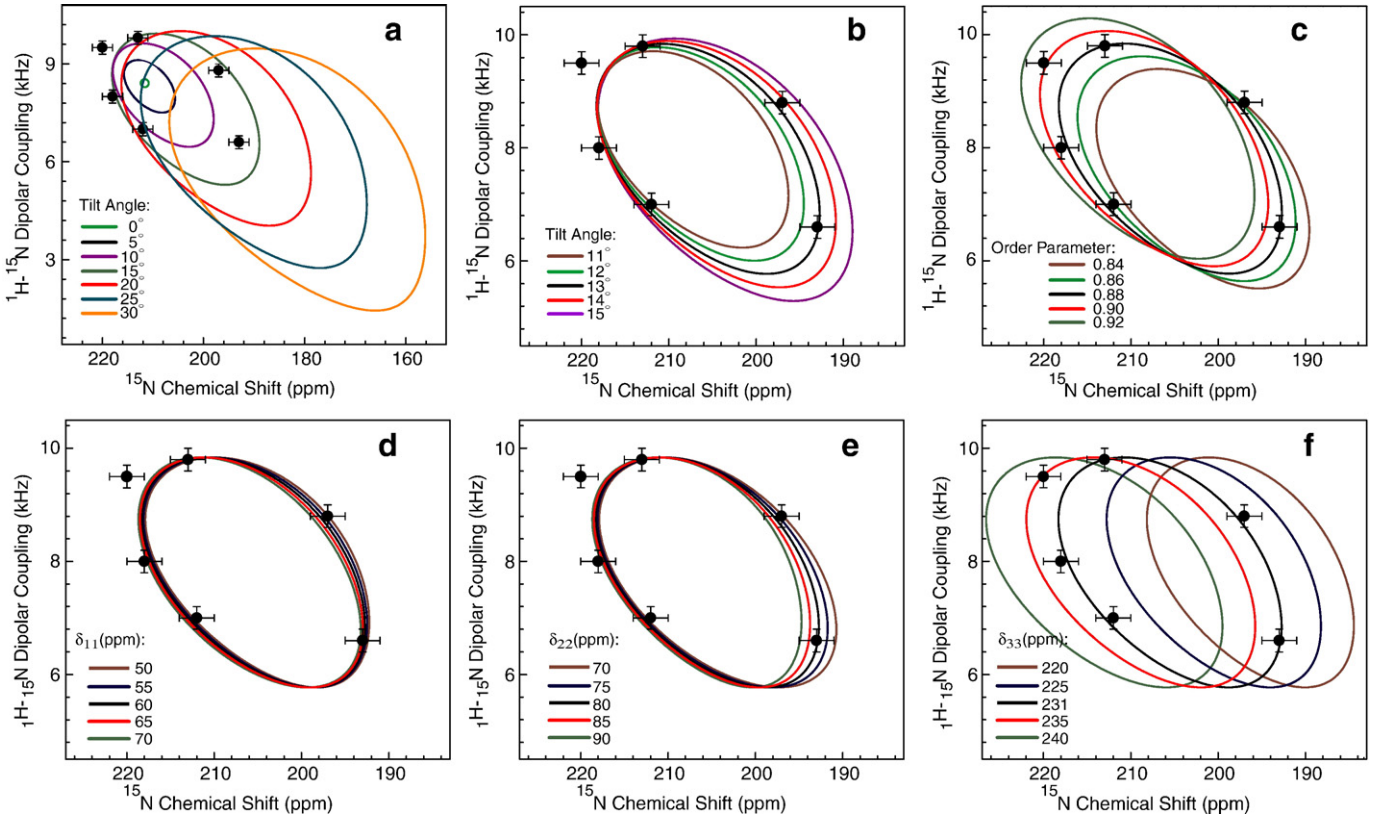

Fig. 7. The dependence of the PISA wheel 2D PISEMA spectrum on (A and B) the tilt angle, (C) order parameter, and (D–F) magnitudes of the principal components of the amide-^{15}N CSA tensor of the TM2 peptide. Experimental data points for each residue were obtained from 2D PISEMA spectra of mechanically aligned POPC bilayers containing the 3 mol% ^{15}N-labeled TM2 peptide at 37 °C.

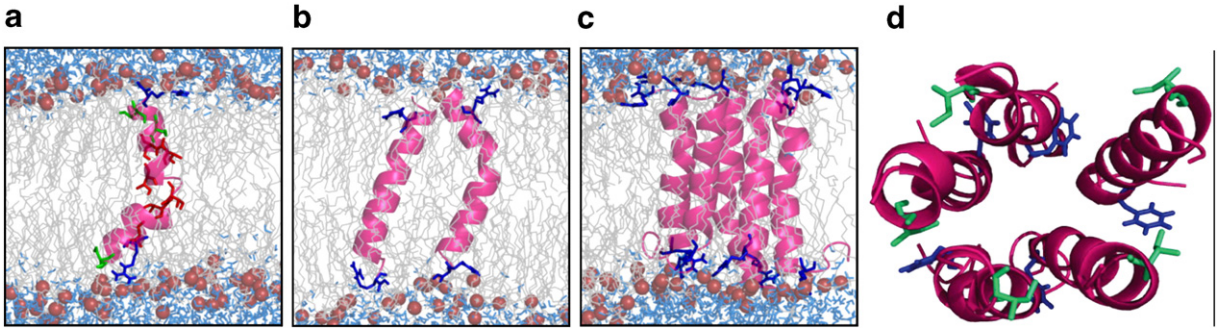

Fig. 8. Snapshots of the monomer (A), dimer (B), side-view of the pentamer (C) and top-view of the pentamer (D) at the end of the simulations, in a DMPC bilayer. The monomer and dimer are destabilized while the pentamer is mostly stable.

thickness nor on the lipid charge. These results also suggest that $GABA_A$-TM2 oligomerizes, with strong peptide–peptide interactions, to form ion-channels in lipid bilayers. This oligomeric form of the peptide most likely overcomes the hydrophobic mismatch between the length of the peptide and the bilayer thickness. To understand the peptide–peptide interactions that stabilize the oligomeric structure of $GABA_A$-TM2, MD simulations were carried and the results are explained below.

3.2.2. Molecular dynamics simulations

MD simulations show that the GABA-TM2 peptide is unstructured in water as predicted by the CD experiments (data not shown). In bilayers, the transmembrane peptide is unstable as a monomer, relatively unstable as a dimer, and mostly stable as a pentamer. The snapshots of the monomer, dimer and pentamer, at the end of the simulations (50 ns), in DMPC bilayers are shown in Fig. 8. The monomer is destabilized, leading to a kink in the middle of the peptide (Fig. 8, top left). The two $GABA_A$-TM2 peptides of the dimeric configuration were placed close to each other (~10 Å apart), but drifted away from each other at the end of the MD simulation (Fig. 8, top right). The pentamer is mostly stable (Fig. 8, bottom). The role of peptide–peptide interactions in the stability of the oligomeric structure is discussed below.

The stability of the peptides is directly related to the nature of the preferred interactions of the hydrophilic residues (Ser, Thr and Arg), which are distributed all along the length of the helix. Thus, in a transmembrane state, these residues are in contact with the interface, lipid head groups or the hydrophobic lipid tails, depending on the position of the specific residue along the sequence. Irrespective of the oligomerization state and lipid bilayer width, Ser-1, Arg-5 and Arg-24 are able to interact with the interfacial region and form stabilizing hydrogen bonds with the lipid head group atoms or interfacial water molecules. The other polar residues are incapable of interacting with the lipid bilayer without significantly disrupting it; but ^{31}P NMR experiments suggest that the TM2 peptide does not alter the lamellar phase bilayer structure. However, these residues are able to form hydrogen bonds with the backbone atoms of the peptide. In a monomer, the Ser and Thr side chains form hydrogen bonds with the carbonyl oxygens in the peptide backbone. This weakens the i–i+4 backbone hydrogen bonds of the helix, leading to a destabilization of the helical structure of the peptide. In an oligomer, while most of the Ser and Thr side chains still form hydrogen bonds with the backbone atoms of the same peptide, some of them form hydrogen bonds with the polar side chains of the neighboring peptide. This intermolecular hydrogen bonding liberates some of the intramolecular hydrogen bonds between the side chains and the backbone, thus strengthening the backbone–backbone hydrogen bonds and stabilizing the peptides (Fig. 9). An example of an intramolecular hydrogen bond is shown in Fig. 9 (left). The backbone carbonyl oxygen of Phe-8 shares a hydrogen bond with the backbone amine (2.86 Å) and side chain –OH (1.63 Å) of Thr-12. In the middle and right frames of Fig. 9, two representative inter-molecular H bonds from a stable pentamer are shown. In the middle frame, a Thr-Ser side chain H-bond (1.9 Å) is shown and in the right frame two Thr residues from two adjacent peptides share a hydrogen bond (1.88 Å). Due to this stabilizing inter-molecular H bonding, the helical structure is not distorted as in the case of a monomer. We find that on an average, each peptide forms ~1.5 intermolecular hydrogen bonds (Fig. 10 and Table 3), and this seems to be sufficient to stabilize both the secondary structure of the individual peptides and the oligomer. The intramolecular hydrogen bonds mentioned in Table 3 and Fig. 10 are between the sidechain residues and the back bone atoms of the peptide. Peptide4 had less number

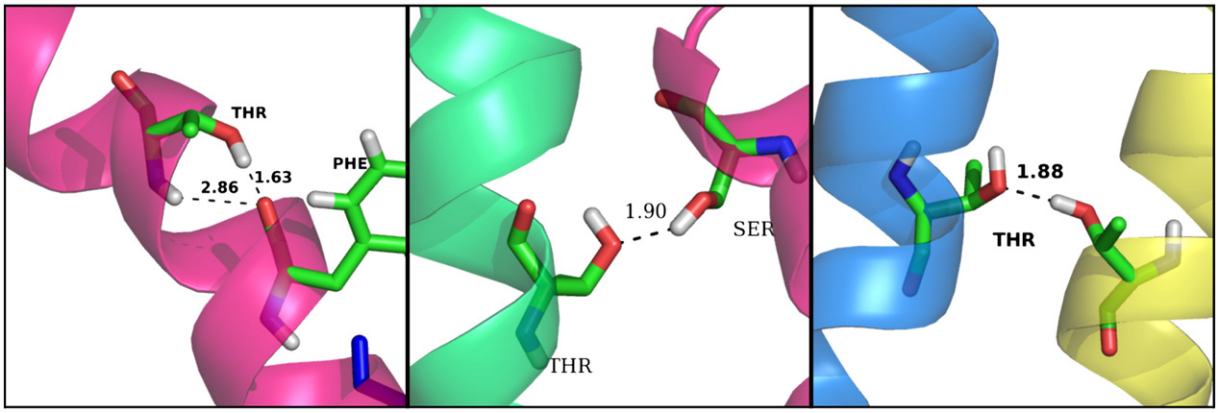

Fig. 9. Representative intra-peptide (left) and inter-peptide (middle and right) H bonds. The inter-peptide H bonds, between the abundant serine and threonine side chains increase the stability of the pentamer.

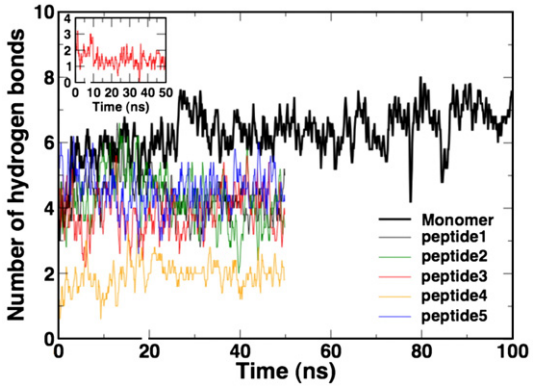

Fig. 10. The number of intramolecular hydrogen bonds (thin lines) of the five peptides in simulation-5 (pentameric $GABA_A$ in DMPC bilayers). The thick black line shows the number of hydrogen bonds in the simulation of the monomer (simulation-1). The inset shows the average number of intermolecular hydrogen bonds per peptide in simulation-5. Also see the details given in Table 3.

of hydrogen bonds only in simulation-5. The numerous (~15 per peptide) intramolecular backbone–backbone hydrogen bonds (not included in Table 3 and Fig. 10) are mostly invariant through the course of the simulations.

The average tilt angle of the peptides in the pentamer is ~14.5° in DMPC bilayers and ~17° in POPC:POPG bilayers (Fig. 11), which is consistent with experimental measurements. While MD simulations reveals that the peptide tilts 2.5° more in thicker POPC:POPG bilayers as compared to the thinner DMPC bilayers to minimize the hydrophobic mismatch effects, such a small difference in the tilt angle lies within NMR experimental errors. Previous studies have shown a large tilt angle difference for other peptides [34–36], which suggests that the peptide–peptide interactions dominate the $GABA_A$-TM2 assembly in an oligomer.

Studies on designed peptides have shown that an introduction of polar interactions in hydrophobic peptides could provide a strong driving force that leads to the assembly of peptides to oligomeric structures in membranes [37]. A recent MD simulation study about the solvation structure of amino acids also suggested that "Ser and Thr are transiently quite stable due to the backbone interaction, yet polar enough to prefer separate hydrogen bonds between residues on aggregated helices when given the opportunity instead of interacting with the backbone" [38]. Our simulations confirm this result, showing that the excessive polar residues, which slightly destabilize the peptide as a monomer, readily form intermolecular hydrogen bonds as oligomers. In the pentamer, whose initial structure was based on a homology model, the putative ion channel is large enough to allow water molecules inside of it, forming a continuous pore. However, during the coarse of the simulation (50 ns long), the pore structure fluctuates, expelling some of the water molecules out of the pore. Nevertheless, some water molecules are always present inside the presumed ion channel. Future simulations with different peptide orientations and channel geometries should yield a clearer picture of water and ion transport through the pore.

Table 3
Number of hydrogen bonds between peptides in the molecular dynamics simulation-5 in DMPC lipid bilayers containing pentameric TM2 helical peptides

	Peptide-1	Peptide-2	Peptide-3	Peptide-4	Peptide-5
Peptide-1	4.1	1.4	0	0	1.4
Peptide-2	1.4	3.9	0.9	0.7	0
Peptide-3	0	0.9	4.0	0.6	0
Peptide-4	0	0.7	0.6	2.0	1.5
Peptide-5	1.4	0	0	1.5	4.6

4. Discussion

The ion-channel activities of $GABA_A$ receptors play important roles in the function of brain and in neurodegenerative diseases [1–4]. It has been shown that the second transmembrane peptide fragment of the $GABA_A$ receptor forms ion channels in planar lipid bilayers [7]. The amino acid sequence of the TM2 segment is nearly identical for various $GABA_A$ subunits (Fig. 2). Studies have shown the importance of the TM2 segment for the function of $GABA_A$ receptor [5,39]. Particularly, point mutation studies have suggested that the Thr and other hydrophilic residues in the TM2 segment play important roles in the selectivity of ions by the $GABA_A$ channel [40,41]. The first structural results presented in this study demonstrate the role of these hydrophilic residues in the structural stability of TM2, which explains why these residues are important in the channel activity. We believe that the reported results would also be valuable in the design of channel-forming peptides. This study also demonstrates the unique advantages of combining solid-state NMR and MD simulation approaches to provide high-resolution insights to understand the functional aspects of challenging transmembrane peptides and proteins. In this study, to better understand the properties of this peptide, we investigated the secondary structure and membrane orientation of the peptide using CD, solid-state NMR spectroscopy and MD simulations. High-resolution solid-state NMR experiments on mechanically aligned lipid bilayers have been successfully used in previous studies to determine the structure and topology of membrane-associated peptides and proteins [12,30,31,42–52].

4.1. Secondary structure

CD experimental results from SUVs and detergent micelles suggest that the TM2 peptide is unstructured in water and forms a helical structure in membrane environments. Further, interatomic distances measured using the REDOR solid-state NMR experiments on MLVs (Fig. 4 and Table 2) suggest that the peptide forms a helical structure in lipid bilayers (Fig. 5). These experimental results are in excellent agreement with MD simulations results.

4.2. Topology, tilt, and oligomeric structure of GABA-TM2 in membrane bilayers

Since the $GABA_A$-TM2 peptide forms ion-channels in planar lipid bilayers, it is important to determine the topology of the peptide at a high-resolution in order to understand the function of the peptide. While previous studies have shown that Ser and Thr can be stable in a hydrophobic environment [53,54], the large number of polar residues in the $GABA_A$-TM2 may force the peptide to prefer a non-

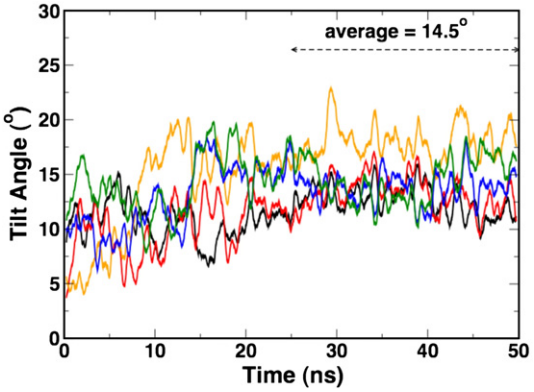

Fig. 11. Tilt angles of individual peptides measured from MD simulations on a pentameric assembly in DMPC bilayers. The tilt angles range from 10° to 19°. But the average value of ~14.5° compares well with the experiments.

transmembrane configuration. To address these ambiguities, we carried out solid-state NMR experiments and MD simulations to measure the orientation of the TM2 peptide in different types of lipid bilayers. The PISA wheel (Fig. 7) generated using the experimentally measured chemical shift and dipolar coupling values (Fig. 6) measured from mechanically aligned bilayers containing TM2 peptides suggest that the peptide has a transmembrane orientation in DMPC, POPC or POPC:POPG lipid bilayers. However, the helical axis of the peptide is tilted away by ~15±2° from the direction of the bilayer normal in all three types of bilayers. These results are in very good agreement with molecular dynamics simulations. Our results suggest that the presence of an anionic lipid, POPG, has no role on the structure and the orientation of the TM2 peptide that has two positively charged Arg residues. This further confirms that the peptide is inserted into the hydrophobic part of the bilayer as it has little affinity for the negative charge on the headgroup of the POPG lipid, which is consistent with the ion-channel activity of the peptide. The measured tilt angle is very similar to that reported from solid-state NMR experiments on melittin in aligned lipid bilayers [55].

Recent studies have shown that hydrophobic mismatch between the hydrophobic length of a helical peptide and the hydrophobic thickness of the lipid bilayer can significantly affect the backbone conformation, membrane-orientation, tilt (the angle between the helical axis and the bilayer normal), and oligomerization of the peptide [34–36,55–63]. It could also lead to changes in the phase, order/disorder, and curvature of lipid bilayers. On the other hand, interestingly the tilt angle and the backbone conformation of the TM2 peptide determined from lipid bilayers with different hydrophobic thickness (for example thinner DMPC bilayer vs thicker POPC bilayers) are similar. Our ^{31}P NMR experiments on MLVs suggested that the lamellar phase bilayer structure of lipids was not perturbed by the presence of TM2 even at a high concentration of 7 mol% TM2. These results suggest that the hydrophobic mismatch does not play a role on the structural folding of the TM2 peptide, and further indicate that the hydrophobic mismatch is most likely compensated by the peptide–peptide interactions. The peptide–peptide interaction was also revealed using MD simulations.

Based on the solid-state NMR experimental results, we assumed that all the peptides are in a transmembrane orientation. Therefore, it is possible in principle to obtain the precise equilibrium oligomeric structure using long MD simulations of randomly distributed peptides in a lipid bilayer. However, the time-scales required for such simulations are prohibitive by current computational standards. Nevertheless, MD simulations were carried out to provide indirect information about the preferred oligomeric state of the peptide by answering questions such as: is the peptide stable as a monomer? If the oligomers are more stable, what are the favorable interactions that stabilize them? Which oligomeric structures generate transmembrane pores so as to enable ion-channel activity? We have limited our MD simulations to address these questions and reported results from different oligomers (monomer, dimer and pentamer) of the GABA-TM2 peptide in DMPC and POPC:POPG bilayers. Simulations revealed intermolecular hydrogen bondings that play a role in the stability of an oligomeric structure and could be on the ion-channel activity of the peptide. It could be interesting to compare the stability of different oligomeric structures (such as trimers, tetramers and pentamers), which is however beyond the scope of the present study. Since the $GABA_A$ protein form pentameric ion-channels, it may not be essential to understand the structures of oligomers beyond pentamers. It would be useful to measure intermolecular distances using REDOR solid-state NMR experiments on fluorinated peptides to determine the oligomeric structure. We believe that the pentameric structural model for the peptide developed in this study will be useful in labeling the peptide for structural studies using solid-state NMR or EPR spectroscopy. In addition, a combination of recently developed solid-state NMR experiments to study the high-resolution structure uniformly-labeled TM2 and MD simulations will provide further insights into the function of the TM2 peptide [64]. It should be noted that while studies on the transmembrane fragment of a membrane protein alone cannot provide complete biophysical and biological insights in to the function of the protein [44,48], several previous studies have demonstrated the value of investigating isolated transmembrane helices of membrane proteins and also the structural and functional correlation between the peptide fragments and the intact proteins [35,36,59,65–67].

Acknowledgement

This research was supported by the research funds from National Institutes of Health (AI054515 to A.R.).

References

[1] F. Da Settimo, S. Taliani, M.L. Trincavelli, M. Montali, C. Martini, GABA(A)/Bz receptor subtypes as targets for selective drugs, Curr. Med. Chem. 14 (2007) 2680–2701.
[2] R.A. Rissman, A.L. De Blas, D.M. Armstrong, GABA(A) receptors in aging and Alzheimer's disease, J. Neurochem. 103 (2007) 1285–1292.
[3] R.L. Macdonald, R.W. Olsen, GABA(A) receptor channels, Annu. Rev. Neurosci. 17 (1994) 569–602.
[4] S.M. Hanson, C. Czajkowski, Structural mechanism underlying benzodiazepine modulation of the GABA(A) receptor, J. Neurosci. 28 (2008) 3490–3499.
[5] M. Xu, M.H. Akabas, Identification of channel-lining residues in the M2 membrane-spanning segment of the GABA(A) receptor alpha(1) subunit, J. Gen. Physiol. 107 (1996) 195–205.
[6] A.K. Bera, M.H. Akabas, Spontaneous thermal motion of the GABA(A) receptor M2 channel-lining segments, J. Biol. Chem. 280 (2005) 35506–35512.
[7] Santos, J. S., Ph.D. Thesis, Biophysics, Univ. of Michigan, Ann Arbor, MI.
[8] S.J. Opella, F.M. Marassi, J.J. Gesell, A.P. Valente, Y. Kim, M. Oblatt-Montal, M. Montal, Structures of the M2 channel-lining segments from nicotinic acetylcholine and NMDA receptors by NMR spectroscopy, Nat. Struct. Biol. 6 (1999) 374–379.
[9] J.H. Chill, J.M. Louis, F. Delaglio, A. Bax, Local and global structure of the monomeric subunit of the potassium channel KcsA probed by NMR, Biochim. Biophys. Acta 1768 (2007) 3260–3270.
[10] T. Gullion, J. Schaefer, Rotational-echo double-resonance NMR, J. Magn. Reson. 81 (1987) 196–200.
[11] C.H. Wu, A. Ramamoorthy, S.J. Opella, High resolution heteronuclear dipolar solid-state NMR spectroscopy, J. Magn. Reson. A109 (1994) 270.
[12] A. Ramamoorthy, Y. Wei, D.K. Lee, PISEMA solid-state NMR spectroscopy, Ann. Rep. NMR Spectrosc. 52 (2004) 1–52.
[13] K.J. Hallock, K.A. Henzler Wildman, D.K. Lee, A. Ramamoorthy, Sublimable solids can be used to mechanically align lipid bilayers for solid-state NMR studies, Biophys. J. 82 (2002) 2499–2503.
[14] G. Metz, X. Wu, S.O. Smith, Ramped-amplitude cross polarization in magic-angle-spinning NMR, J. Magn. Reson. A 110 (1994) 219–227.
[15] A.E. Bennet, C.M. Rienstra, M. Auger, K.V. Lakshmi, R.G. Griffin, Heteronuclear decoupling in rotating solids, J. Chem. Phys. 103 (1995) 6951–6958.
[16] M. Lee, W.I. Goldburg, Nuclear-magnetic-resonance line narrowing by a rotating RF field, Phys. Rev. 140 (1965) 1261.
[17] A. Ramamoorthy, C.H. Wu, S.J. Opella, Experimental aspects of multidimensional solid-state NMR correlation spectroscopy, J. Magn. Reson. 140 (1999) 131–140.
[18] K. Yamamoto, D.K. Lee, A. Ramamoorthy, Broadband-PISEMA solid-state NMR spectroscopy, Chem. Phys. Lett. 407 (2005) 289–293.
[19] C.D. Schwieters, J.J. Kuszewski, N. Tjandra, G.M. Clore, The Xplor-NIH NMR molecular structure determination package, J. Magn. Reson. 160 (2003) 65–73.
[20] M. Nilges, A.M. Gronenborn, A.T. Brunger, G.M. Clore, Determination of three-dimensional structures of proteins by simulated annealing with inter-proton distance constraints. Application to crambin, Potato carboxypeptidase inhibitor and Barley serine protease inhibitor 2, Protein Eng. 2 (1988) 27–38.
[21] R. Koradi, M. Billeter, K. Wuthrich, MOLMOL: a program for display and analysis of macromolecular structures, J. Mol. Graphics. 14 (1996) 51–55.
[22] E. Lindahl, B. Hess, D. Van der Spoel, GROMACS 3.0: a package for molecular simulation and trajectory analysis, J. Mol. Model. 7 (2001) 306–317.
[23] D. Van der Spoel, E. Lindahl, B. Hess, G. Groenhof, A.E. Mark, H.J. Berendsen, GROMACS: fast, flexible, and free, J. Comput. Chem. 26 (2005) 1701–1718.
[24] O. Berger, O. Edholm, F. Jahnig, Molecular dynamics simulations of a fluid bilayer of dipalmitoylphosphatidylcholine at full hydration, constant pressure, and constant temperature, Biophys. J. 72 (1997) 2002–2013.
[25] J.D. Faraldo-Gomez, G.R. Smith, M.S.P. Sansom, Setting up and optimization of membrane protein simulations, Eur. Biophys. J. 31 (2002) 217–227.
[26] M. O'Mara, B. Cromer, M. Parker, S.H. Chung, Homology model of the GABA(A) receptor examined using Brownian dynamics, Biophys. J. 88 (2005) 3286–3299.
[27] H. Saito, Conformation-dependent ^{13}C chemical shifts — a new conformational characterization as obtained by high-resolution solid-state ^{13}C NMR, Magn. Res. Chem. 24 (1986) 835–852.
[28] D.K. Lee, A. Ramamoorthy, Determination of the solid-state conformations of polyalanine using magic-angle spinning NMR spectroscopy, J. Phys. Chem. B 103 (1999) 271.

[29] J.D. Gehman, F. Separovic, K. Lu, A.K. Mehta, Boltzmann statistics rotational-echo double-resonance analysis, J. Phys. Chem. B 111 (2007) 7802–7811.
[30] F.M. Marassi, S.J. Opella, A solid-state NMR index of helical membrane protein structure and topology, J. Magn. Reson. 144 (2000) 150–155.
[31] J. Wang, J. Denny, C. Tian, S. Kim, Y. Mo, F. Kovacs, Z. Song, K. Nishimura, Z. Gan, R. Fu, J.R. Quine, T.A. Cross, Imaging membrane protein helical wheels, J. Magn. Reson. 144 (2000) 162–167.
[32] Y. Wei, D.H. Lee, A. Ramamoorthy, A two-dimensional magic angle decoupling and magic angle turning solid-state NMR method — an application to study chemical shift tensors from peptides that are non-selectively labeled with ^{15}N isotope, J. Phys. Chem. B, 104 (2001) 4752–4762.
[33] A. Poon, J. Birn, A. Ramamoorthy, Variation of Amide-^{15}N Chemical Shift Tensors in Proteins, J. Phys. Chem. B 108 (2004) 16577.
[34] S.H. Park, S.J. Opella, Tilt angle of a trans-membrane helix is determined by hydrophobic mismatch, J. Mol. Biol. 350 (2005) 310–318.
[35] F.A. Kovacs, T.A. Cross, Transmembrane four-helix bundle of influenza A M2 protein channel: structural implications from helix tilt and orientation, Biophys. J. 73 (1997) 2511–2517.
[36] A. Ramamoorthy, S.K. Kandasamy, D.K. Lee, S. Kidambi, R.G. Larson, Topology and tilt of cell-signaling peptides containing nuclear localization sequences in membrane bilayers determined by solid-state NMR and molecular dynamics simulation studies, Biochemistry 46 (2007) 965–975.
[37] C.D. Tatko, V. Nanda, J.D. Lear, W.F. Degrado, Polar networks control oligomeric assembly in membranes, J. Am. Chem. Soc. 128 (2006) 4170–4171.
[38] A.C.V. Johansson, E. Lindahl, Amino-acid solvation structure in transmembrane helices from molecular dynamics simulations, Biophys. J. 91 (2006) 4450–4463.
[39] M. Xu, M.H. Akabas, Amino-acids lining the channel of the gamma-aminobutyric-acid type-A receptor identified by cysteine substitution, J. Biol. Chem. 268 (1993) 21505–21508.
[40] J.E. Dalziel, B. Birnir, A.B. Everitt, M.L. Tierney, G.B. Cox, P.W. Gage, A threonine residue in the M2 region of the beta(1) subunit is needed for expression of functional alpha(1)beta(1) GABA(A) receptors, Eur. J. Pharmacol. 370 (1999) 345–348.
[41] S. Ueno, A. Lin, N. Nikolaeva, J.R. Trudell, S.J. Mihic, R.A. Harris, N.L. Harrison, Tryptophan scanning mutagenesis in TM2 of the GABA(A) receptor alpha subunit: effects on channel gating and regulation by ethanol, Br. J. Pharmacol. 131 (2000) 296–302.
[42] B.A. Cornell, F. Separovic, A.J. Baldassi, R. Smith, Conformation and orientation of gramicidin-A in oriented phospholipids bilayers measured by solid-state ^{13}C NMR, Biophys. J. 53 (1988) 67–76.
[43] J.R. Quine, T.A. Cross, Protein structure in anisotropic environments: unique structural fold from orientational constraints, Concep. Magn. Reson. 12 (2000) 71–82.
[44] U.H.N. Dürr, L. Waskell, A. Ramamoorthy, The cytochromes P450 and b(5) and their reductases — promising targets for structural studies by advanced solid-state NMR spectroscopy, BBA Biomembranes 1768 (2007) 3235–3259.
[45] M. Kamihira, T. Vosegaard, A.J. Mason, S.K. Straus, N.C. Nielsen, A. Watts, Structural and orientational constraints of bacteriorhodopsin in purple membranes determined by oriented-sample solid-state NMR spectroscopy, J. Struct. Biol. 149 (2005) 7–16.
[46] S. Abu-Baker, J.X. Lu, S. Chu, K.K. Shetty, P.L. Gor'kov, G.A. Lorigan, The structural topology of wild-type phospholamban in oriented lipid bilayers using N-15 solid-state NMR spectroscopy, Prot. Sci. 16 (2007) 2345–2349.
[47] C. Aisenbrey, M. Cusan, S. Larnbotte, P. Jasperse, J. Georgescu, U. Harzer, B. Bechinger, Specific isotope labeling of colicin E1 and B channel domains for membrane topological analysis by oriented solid-state NMR spectroscopy, Chem. Bio. Chem. 9 (2008) 944–951.
[48] U.H.N. Dürr, K. Yamamoto, S.C. Im, L. Waskell, A. Ramamoorthy, Solid-state NMR reveals structural and dynamical properties of a membrane-anchored electron-carrier protein, cytochrome *b*(5), J. Am. Chem. Soc. 129 (2007) 6670–6671.
[49] N.J. Traaseth, R. Verardi, K.D. Torgersen, C.B. Karim, D.D. Thomas, G. Veglia, Spectroscopic validation of the pentameric structure of phospholamban, Proc. Natl. Acad. Sci. USA 37 (2007) 14676–14681.
[50] E. Strandberg, P. Wadhwani, O. Tremouilhac, U.H.N. Durr, A.S. Ulrich, Solid-state NMR analysis of the PGLa peptide orientation in DMPC bilayers: structural fidelity of H-2-labels versus high sensitivity of F-19-NMR, Biophys. J. 90 (2006) 1676–1686.
[51] F. Porcelli, B. Buck, D.K. Lee, K.J. Hallock, A. Ramamoorthy, G. Veglia, Structure and orientation of Pardaxin determined by NMR experiments in model membranes, J. Biol. Chem. 279 (2004) 45815–45823.
[52] A. Ramamoorthy, S. Thennarasu, D.K. Lee, A. Tan, L. Maloy, Solid-state NMR investigation of the membrane-disrupting mechanism of antimicrobial peptides MSI-78 and MSI-594 derived from Magainin 2 and Melittin, Biophys. J. 91 (2006) 206–216.
[53] T.M. Gray, B.W. Matthews, Intra-helical hydrogen-bonding of serine, threonine and cysteine residues within alpha-helices and its relevance to membrane-bound proteins, J. Mol. Biol. 175 (1984) 75–81.
[54] J.P. Dawson, J.S. Weinger, D.M. Engelman, Motifs of serine and threonine can drive association of transmembrane helices, J. Mol. Biol. 316 (2002) 799–805.
[55] R. Smith, F. Separovic, T.J. Milne, A. Whittaker, F.M. Bennett, B.A. Cornell, A. Markriyannis, Structure and orientation of the pore-forming peptide, melittin, in lipid bilayers, J. Mol. Biol. 241 (1994) 456–466.
[56] S.H. White, W.C. Wimley, Hydrophobic interactions of peptides with membrane interfaces, Biochim. Biophys. Acta. 1376 (1998) 339–352.
[57] Y.P. Zhang, R.N. Lewis, R.S. Hodges, R.N. McElhaney, Interaction of a peptide model of a hydrophobic transmembrane alpha-helical segment of a membrane protein with phosphatidylcholine bilayers: differential scanning calorimetric and FTIR spectroscopic studies, Biochemistry, 31 (1992) 11579–11588.
[58] E. Strandberg, S. Ozdirekcan, D.T.S. Rijkers, C.A. Val der Wel, R.E. Koepee II, R.M.J. Liskamp, J.A. Killian, Tilt angles of transmembrane model peptides in oriented and non-orientated lipid bilayers as determined by 2H solid-state NMR, Biophys. J. 86 (2004) 3709–3721.
[59] F.A. Kovacs, J.F. Denny, Z. Song, J.R. Quine, J.A. Cross, Helix tilt of the M2 transmembrane peptide from influenza A virus: an intrinsic property, J. Mol. Biol. 295 (2000) 117–125.
[60] U. Harzer, B. Bechinger, Alignment of lysine-anchored membrane peptides under conditions of hydrophobic mismatch: a CD, ^{15}N and ^{31}P solid-state NMR spectroscopy investigation, Biochemistry, 39 (2000) 13106–13114.
[61] K.J. Hallock, D. Lee, J. Omnaas, H.I. Mosberg, A. Ramamoorthy, Membrane composition determines Pardaxin's mechanism of lipid bilayer disruption, Biophys. J. 83 (2002) 1004–1013.
[62] M.R.R. de Planque, D.T.S. Rijkers, J.I. Fletcher, R.M.J. Liskamp, F. Separovic, The alpha-M1 segment of the nicotinic acetylcholine receptor exhibits conformational flexibility in a membrane environment, BBA Biomembranes 1665 (2004) 40–47.
[63] M.R.R. de Planque, D.T.S. Rijkers, R.M.J. Liskamp, F. Separovic, The alpha-M1 segment of the nicotinic acetylcholine receptor interacts strongly with model membranes, Magn. Res. Chem. 42 (2004) 148–154.
[64] A. Ramamoorthy (Ed.), NMR Spectroscopy of Biological Solids, Taylor & Francis, New York, 2006.
[65] K.R. MacKenzie, J.H. Prestegard, D.M. Engelman, A transmembrane helix dimmer: structure and implications, Science 276 (1977) 131–133.
[66] T. Cohen, M. Pevsner-Fischer, N. Cohen, I.R. Cohen, Y. Shai, Characterization of the interacting domain of the HIV-1 fusion peptide with the transmembrane domain of the T-cell receptor, Biochemistry 47 (2008) 4826–4833.
[67] R.F.M. De Almeida, L.M.S. Loura, M. Prieto, A. Watts, A. Fedorov, F.J. Barrantes, Structure and dynamics of the gamma M4 transmembrane domain of the acetylcholine receptor in lipid bilayers: insights into receptor assembly and function, Mol. Mem. Biol. 23 (2006) 305–315.